Structural Engineering

INTERSECTII
INTERSECTIONS
http://www.ce.tuiasi.ro/intersections

# Nonlinear Analysis of Reinforced Concrete Frames

Jeovan Faleiro, Alex Barbat and Sergio Oller
*Escuela Técnica Superior de Ingenieros de Caminos, Canales y Puertos, Techinical University of Catolonia, 08034, Barcelona Spain*

## Summary

*This paper develops an improved analytical model for predicting the damage response of multi-storey reinforced concrete frames modeled as an elastic beam-column with two inelastic hinges at its ends. The damage is evaluated in the hinges, using the concentrated damage concepts and a new member damage evaluation method for frame members, which leads to a meaningful global damage index of the structure. A numerical procedure for predicting the damage indexes of the structures using matrix structural analysis, plastic theory and continuum damage model is also developed. The method is adequate for the prediction of the failure mechanisms. Numerical examples are finally included*

KEYWORDS: Damage estimation; Global damage; Plastic-damage model; Reinforced concrete frames.

## 1. INTRODUCTION

The constitutive models based on the Continuum Damage Mechanics and the development of the numerical techniques enables to retake existing structural models and improve their capacity of evaluating the global damage state of reinforced concrete building. Plastic theory can be used as mathematical framework to treat permanent strains. However, in particular geomaterials, such as concrete, permanent strains are caused by microcracking, what leads to permanent stiffness degradation. In those cases, the plasticity theory itself is not satisfactory to represent the stiffness degradation, and therefore it is necessary to use another tool, the Continuum Damage Mechanics.

Using the works of Kachanov (1958), Continuum Damage Mechanics became one of the most studied subjects in Solids Mechanics. The main idea is defining a new damage internal variable which describes the evolution of microcracks and microvoids and their influence on the behavior of the material. This simple and general idea has been used for modelling, until the local fracture, most of the construction materials. Initially introduced for metals, the Continuum Damage Mechanics was later adapted to materials such as concrete (Oller 2001). Currently

ISSN 1582-3024

there are some models in which plasticity and damage are coupled (Simo and Ju 1987; Lucciomi et al. 1996). This approach has the advantage of allowing the development of constitutive independent laws which simulate materials in which the plastic deformation is not significant, as in the case of concrete, ceramic and ceramic composites.

Nowadays, Continuum Mechanics is still not the most suitable analysis framework for certain civil engineering structures, like framed structures which are usually modelled by means of bar elements, while continuum mechanics is used mostly in the case of finite elements models of the structure. Perhaps the main inconvenience in the use of finites elements consists in the fact that the most of the results obtained will be useless or of little practical utility for the structural designer. In this article we use the computational advantages of the matrix formulation for framed building structures, together with the complexity of the plastic-damage constitutive models.

Nonetheless, plasticity theory has been successfully adapted to frame analysis using the concept of lumped plasticity models, in which it is assumed that plastic effects can be concentrated at special locations called plastic hinges. This approach can be justified since in frame analysis the deformation is usually concentrated at or very near the end of the beams, and these are the only results of the frames analysis usually used by the structural designer.

Using the lumped plasticity model, Cipollina et al. (1995) and Flórez-López (1995) adapted the damage models to frame analysis in which the damage is concentrated on plastic hinges, the concentrated damage model. A value of the concentrated damage at the hinge equal to 1 reflects complete loss of strength while a value 0 means no damage. However, this method has the inconvenient that only refers to the damage at the hinge, and do not take into account the effect of cumulative plastic deformations under cyclic loading. Another inconvenient is that, once the concentrated damage index is located at the end of the frame member, is not possible to determine the real damage state of the member.

Based on method proposed by Hanganu et al. (2002), we will present one global damage evaluation method based on continuum mechanics principles in which the label "member damage" will be applied only to damage indices describing the state of frame member while the "global" damage indices will refers to state of whole structure. Both damage indices, member and global, presented herein are independently from the chosen constitutive models for the structural material.

This feature converts the proposed member and global damage indices into a powerful general tool for structural assessment. Moreover, it is applicable directly to both static and dynamic analysis and to estimate the damage produced by seismic actions in reinforced concrete building structures.

Structural Engineering

INTERSECTII
INTERSECTIONS
http://www.ce.tuiasi.ro/intersections

J. Faleiro, A. Barbat, S. Oller

This paper will describe the procedure to use plastic-damage models in frame analysis, with application to reinforced concrete structures, in accordance with the classic theories of Continuum Damage Mechanics and classic theories of plasticity. These theories will give support to the implementation of the member and global damage indices. What distinguishes this work from others is the fact the complete plastic-damage constitutive model, as well as the global damage, is here implemented into a frame analysis algorithm, which is briefly outlined. Finally, we will validate the method trough analysis of framed structures, as a single story bay frame structure, a simply supported reinforced concrete beam, and by a 2 story bay reinforced concrete frame structure.

## 2. BASIC DEFINITIONS

Let us consider a plane frame with $b$ elements, connected into $n$ nodes. The displacement of the structure is studied during a time interval $[0,T]$. At time $t=0$ the state of the structure is denoted as 'initial or undeformed configuration'. The configuration of the structure will be called 'deformed' for any $t>0$. As a reference, we will consider a couple of orthogonal coordinate axes $X$ and $Y$ to define the position of each node in any configuration. During the deformation of the structure, this coordinate system is assumed to be stationary.

Beams or columns extremities define the frame elements, where joints $i$ and joint $j$ indicate an element. Conventionally, the direction of each element is defined by the $i-j$ nodes. Each joint has three degrees of freedom. For example, the generalized nodal displacement in a node $i$ s can be defined as $\{\mathbf{u}_i\}^\mathbf{T} = \{q_1 \quad q_2 \quad q_3\}$, where $q_1, q_2$ and $q_3$ indicate the node displacement in the directions $X$ and Y, and the node rotation with respect to the initial configuration, respectively. In this article $\{\bullet\}$ indicates a column matrix and $[\bullet]$ indicates a quadratic matrix.

For each element $b$, the generalized displacement vector for nodes $i-j$ can be defined as $\{\mathbf{q}_b\}^\mathrm{T} = \{\mathbf{u}_i^\mathrm{T} \quad \mathbf{u}_j^\mathrm{T}\} = \{q_1 \quad q_3 \quad q_2 \quad q_4 \quad q_5 \quad q_6\}$ and the global displacement $\{\mathbf{U}\}$ of the structure is

$$\{\mathbf{U}\}^\mathrm{T} = \{\mathbf{u}_1^\mathrm{T} \quad \mathbf{u}_2^\mathrm{T} \quad .... \quad \mathbf{u}_n^\mathrm{T}\} \tag{1}$$

The generalized deformations $\{\mathbf{\Phi}_b\}$ of the beam $b$ can be defined as

$$\{\mathbf{\Phi}_b\}^\mathrm{T} = \{\phi_i \quad \phi_j \quad \delta\} \tag{2}$$

Structural Engineering

INTERSECTII
INTERSECTIONS
http://www.ce.tuiasi.ro/intersections



where $\phi_i$ and $\phi_j$ indicate rotations of the member at the ends $i$ and $j$ respectively and $\delta$ is its elongation.

The generalized deformations $\{\mathbf{\Phi}_b\}$ can be expressed in terms of the global displacement $\{\mathbf{U}\}$ by

$$\{\mathbf{\Phi}_b\} = [\mathbf{B}_b]\{\mathbf{U}\} \tag{3}$$

where $[\mathbf{B}_b]$.is the global displacement transformation matrix.

The generalized "effective" stress vector of the frame element $b$ is defined as

$$\{\mathbf{M}_b\}^{\mathrm{T}} = \{m_i \quad m_j \quad n\} \tag{4}$$

which contains the final forces of the member, where $m_i$ and $m_j$ are the moments at the ends of the member and $n$ indicates the axial force. The internal force is the sum of all generalized effective stress $\{\mathbf{M}_b\}$

$$\{\mathbf{F}_{int}\} = \sum_{b=1}^{3n} [\mathbf{B}_b]^{\mathrm{T}} \{\mathbf{M}_b\} \tag{5}$$

The structure is subject to concentrated forces and moments only on the nodes, grouped into a vector $\{\mathbf{F}_{ext}\}$

$$\{\mathbf{F}_{ext}\}^{\mathrm{T}} = \{ \underbrace{f_1, f_2, f_3}_{\text{forces on node 1}} \quad ..... \quad \underbrace{f_{3n-2}, f_{3n-1}, f_{3n}}_{\text{forces on node } n} \} \tag{6}$$

Using now the expressions of the inertial and internal forces, the equation of quasi-static equilibrium of the nodes is expressed as:

$$\{\mathbf{F}_{ext}\} - \{\mathbf{F}_{int}\} = 0 \tag{7}$$

The relation between generalized stress and the history of deformations can be expressed as follows:

$$\{\mathbf{M}_b\} = [\mathbf{S}_b^e(\mathbf{\Phi}_b)]\{\mathbf{\Phi}_b\} \text{ or } \{\mathbf{\Phi}_b\} = [\mathbf{F}_b^e(\mathbf{M}_b)]\{\mathbf{M}_b\} \tag{8}$$

where $[\mathbf{S}_b^e(\mathbf{\Phi}_b)]$ and $[\mathbf{F}_b^e(\mathbf{M}_b)]$ indicate the local elastic stiffness and flexibility matrices, respectively. They are defined according to the deformed configuration of the member.

In the case of small deformations, the elastic stiffness and flexibility matrices remain constant. In this context, the equation (8) can be rewritten as

$$[\mathbf{M}_b] = [\mathbf{S}_b^e]\{\mathbf{\Phi}_b\} \text{ or } \{\mathbf{\Phi}_b\} = [\mathbf{F}_b^e]\{\mathbf{M}_b\} \tag{9}$$

ISSN 1582-3024

Structural Engineering
INTERSECTII
INTERSECTIONS
http://www.ce.tuiasi.ro/intersections



with $[\mathbf{S}_b^e] = [\mathbf{F}_b^e]^{-1}$ being the stiffness elastic matrix.

Inserting equation (9) into (7) and expanding the expression as a function of displacements:

$$\underbrace{\left(\sum_{b=1}^{nelements} [\mathbf{B}_b]^{\mathrm{T}} : [\mathbf{S}_b] : [\mathbf{B}_b]\right) : \{\mathbf{U}\}}_{Internal\ Force} = \{\mathbf{F}_{ext}\} \tag{10}$$

$\sum[\mathbf{B}_b^{\mathrm{T}}] : [\mathbf{S}_b^e] : [\mathbf{B}_b] = [\mathbf{K}^e]$ is the global stiffness matrix.

## 3. CONCENTRATED PLASTICITY APPROACH FOR FRAME MEMBERS

For many reinforced concrete cross sectional shapes, the spread of plasticity starting from the ends of the members along the length is not very significant, and the deformation is concentrated at or very near the cross sections of the ends (Deierlein 2001). Therefore, we will assume that all the plasticity is concentrated at the end cross section. We also assume that the plastification of the end cross section is sudden, rather than gradual or fiber-by-fiber, and that the material behaves in a perfectly elastic plastic manner.

### 3.1. Lumped plasticity model

A constitutive equation can be obtained relating the generalized stress $\{\mathbf{M}_b\}$ with the generalized deformations $\{\mathbf{\Phi}_b\}$ by using the 'lumped dissipation model, considering plasticity, hardening or any other energy dissipation. Energy dissipation is assumed to be concentrated only at the hinges, while beam-column behavior always remains elastic. With these concepts, we can express the member deformations as:

$$\{\mathbf{\Phi}_b\} = [\mathbf{F}_b^e] : \{\mathbf{M}_b\} + \{\mathbf{\Phi}_b^p\} \tag{11}$$

The term $[\mathbf{F}_b^e] : \{\mathbf{M}_b\} = \{\mathbf{\Phi}^e\}$ corresponds to the beam-column elastic deformations, while $\{\mathbf{\Phi}_b^p\}$ is called 'plastic hinge deformations':

$$\{\mathbf{\Phi}_b^p\}^{\mathrm{T}} = \{\phi_i^p \quad \phi_j^p \quad \delta^p\} \tag{12}$$

where $\phi_i^p$ and $\phi_j^p$ represent the plastic rotations of the member at the ends $i$ and $j$ respectively, and $\delta^p$ is its plastic elongation.

ISSN 1582-3024

Structural Engineering

INTERSECTII
INTERSECTIONS
http://www.ce.tuiasi.ro/intersections



Using the generalized stress $\{\mathbf{M}_b\}$ from the equation (11), we will obtain:

$$\{\mathbf{M}_b\} = [\mathbf{S}_b^e] : \left(\{\mathbf{\Phi}_b\} - \{\mathbf{\Phi}_b^p\}\right) \tag{13}$$

Equation (13), assumes that plastic hinges produce when the load on structure increases, until the structure becomes unstable (or a mechanism) due to the development of various plastic hinges. Once a mechanism formed, the structure continues to deform until the final instability is detected by the singularity of the global stiffness matrix.

## 3.2. Internal variable evolution laws and plastic functions

For the internal variables defined in Equation(12), the plastic deformation evolution laws (Cipollina et al. 1995) is:

$$\begin{aligned} &\dot{\phi}_i^p = \dot{\lambda}_i^p \frac{\partial f_i}{\partial m_i} \quad \dot{\phi}_j^p = \dot{\lambda}_j^p \frac{\partial f_j}{\partial m_j} \\ &\dot{\delta}^p = \dot{\lambda}_i^p \frac{\partial f_i}{\partial n} + \dot{\lambda}_j^p \frac{\partial f_j}{\partial n} \end{aligned} \tag{14}$$

where $f_i \le 0$ and $f_j \le 0$ are the yield functions of hinges $i$ and $j$, respectively. These functions depend on the generalized stress $\{\mathbf{M}_b\}$ and also depend on the internal variables and plastic multipliers $\dot{\lambda}_i^p$ and $\dot{\lambda}_j^p$. The plastic multipliers according to the Kuhn-Tucker conditions are:

$$\text{No plasticity} \begin{cases} \dot{\lambda}_i^p = 0 \text{ if } f_i < 0 \quad \text{or} \quad \lambda_i^p \dot{f}_i < 0 \\ \dot{\lambda}_j^p = 0 \text{ if } f_j < 0 \quad \text{or} \quad \lambda_j^p \dot{f}_j < 0 \end{cases} \tag{15}$$

$$\text{Plasticity increment} \begin{cases} \dot{\lambda}_i^p \ne 0 \text{ if } f_i = 0 \text{ and } \lambda_i^p \dot{f}_i = 0 \\ \dot{\lambda}_j^p \ne 0 \text{ if } f_j = 0 \text{ and } \lambda_j^p \dot{f}_j = 0 \end{cases} \tag{16}$$

To plastic multiplier strictly positive, we will consider that the plastic deformation is ‘active’; otherwise it will be called ‘passive’.

### *3.2.1. Plastic functions*

The yield criterion or plastic function at any end is usually a function of the bending moment at the end cross section. Simple plastic functions for initial yield may be of the following type:

$$f_i(m_i) = |m_i| - m_y \le 0 \qquad f_j(m_j) = |m_j| - m_y \le 0 \tag{17}$$

where $m_y$ is the yield moment or plastic moment..

For those cases where the influence of the force is considered, the yield function proposed by Argyris et al. (1982) is:

$$f_i(m_i) = \frac{|m_i|}{m_y} + \left(\frac{n}{n_y}\right)^2 - \alpha \leq 0 \qquad f_j(m_j) = \frac{|m_j|}{m_y} + \left(\frac{n}{n_y}\right)^2 - \alpha \leq 0 \qquad (18)$$

where $n_y$ is the yield force limit (see Figure 1).

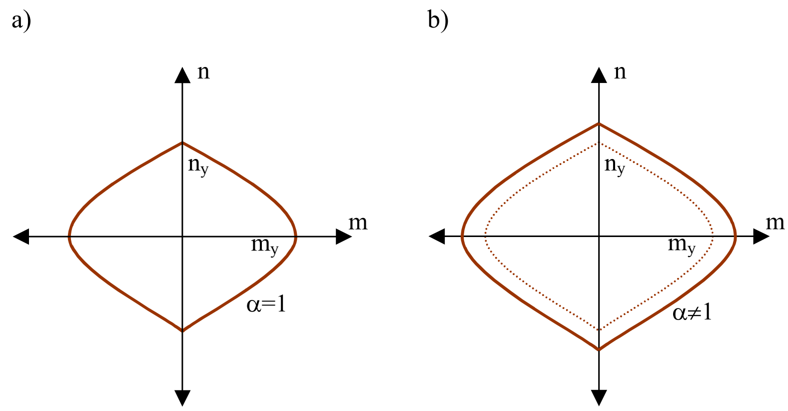


Figure 1. Yield Surface in m-n space: a) without hardening, b) with hardening

It is also possible to describe yield functions that take hardening or softening into account. For example, if we consider the hardening as functions of the plastic rotations of the member, Equation (17) can be rewritten as (Flórez-López 1999):

$$f_i(m_i) = \left|m_i - c\phi_i^p\right| - m_y \leq 0 \qquad f_j(m_j) = \left|m_j - c\phi_j^p\right| - m_y \leq 0 \qquad (19)$$

where $c$ is a constant which indicates a material characteristic.

Despite the fact that the yield surface is the same for the hinges *i* and *j*, the plastic multipliers are independent of each other. This indicates the possibility that for the same element, one of the extremities is being plastified while the other extremity is not. However, the equilibrium at the nodes must be verified by equation (7), which requires the use of some interactive method, such as the Newton-Raphson method, in order to be solved.

## 4. CONTINUOUS DAMAGE MODEL

We will review some basic concepts of continuum mechanics necessary for the subsequent development of the concentrated damage concepts (Simo and Ju 1987).

Physically, degradation of the material properties is the result of the initiation, growth, and coalescence of microcracks or microvoids. Within the context of continuum mechanics, one may model this process by introducing an internal damage variable that can be a scalar or a tensorial quantity.

Let us consider $\mathbf{C}$, a fourth-order tensor, which characterizes the state of damage and transforms the homogenized tensor $\boldsymbol{\sigma}$ into the effective stress tensor $\bar{\boldsymbol{\sigma}}$ (or vice versa), clearly:

$$\bar{\boldsymbol{\sigma}} = \mathbf{C}^{-1} : \boldsymbol{\sigma} \tag{20}$$

For the isotropic damage case, the mechanical behavior of microcracks or microvoids is independent of their orientation, and depends only on a scalar variable $d$. For that reason, $\mathbf{C}$ will simply reduce to $\mathbf{C} = (1-d)\mathbf{I}$, where $\mathbf{I}$ is the rank four-identity tensor, and equation (20) becomes:

$$\bar{\boldsymbol{\sigma}} = \frac{\boldsymbol{\sigma}}{(1-d)} \tag{21}$$

where $d$ is the damage parameter, $\boldsymbol{\sigma}$ the Cauchy stress tensor and $\bar{\boldsymbol{\sigma}}$ is the effective stress tensor, both at time $t$. Here, $d \in (0,1]$ is a given constant.

The coefficient $1-d$ dividing the stress tensor in equation (21) is a *reduction factor* associated with the amount of damage in the material, initially introduced by Kachanov. The value $d=0$ corresponds to the undamaged state, whereas a value $d=1$ corresponds to a *damaged* state. The value $d=1$ defines complete local rupture. Another possible interpretation is that physically the damage parameter $d$ is the ratio of damage surface area over total (nominal) surface area at a local material point.

### 4.1. Flexibility matrix of damaged member

Considering the existence of variables, which represent the concentrated damage at the $b$ frame element, which can be defined as (Flórez-López 1993; Faleiro 2004)

$$\{\mathbf{D}\}^T = \{d_i \quad d_j \quad d_a\} \tag{22}$$

where $d_i$ and $d_j$ are a measure of the bending concentrated damage of hinges $i$ and $j$, respectively, and $d_a$ indicates the measure of axial damage of the member.

These variables can take values between zero, no damage, and one, completely damaged. In the same way as the plasticity, we define that all bending concentrated damage parameters are concentrated at the nodes.

Now, supposing existence of a flexibility matrix of a damaged member $\{\mathbf{F}^d\}$, we have (Faleiro 2005)

$$\underbrace{\{\boldsymbol{\Phi}_b\} = [\mathbf{F}_b^d]\{\mathbf{M}_b\}}_{\begin{Bmatrix}\phi_i\\ \phi_j\end{Bmatrix}=\begin{bmatrix}f_{11} & f_{12}\\ f_{21} & f_{22}\end{bmatrix}\begin{Bmatrix}m_i\\ m_j\end{Bmatrix}} \tag{23}$$

$$[\mathbf{F}^d] = \frac{L}{6EI}\begin{bmatrix}\dfrac{2}{(1-d_i)} & -1\\ -1 & \dfrac{2}{(1-d_j)}\end{bmatrix} \tag{24}$$

$[\mathbf{F}^d]$ represents the flexibility matrix of a damaged member and its inverse is the stiffness matrix of a damaged member $[\mathbf{S}^d]=[\mathbf{F}^d]^{-1}$. If we also include the axial damage influence and redefine the stiffness matrix as a function of concentrated damage vector $\{\mathbf{D}_b\}$ for a element $b$, in small displacements, we have (Faleiro 2005)

$$[\mathbf{S}_b^d(\mathbf{D}_b)] = \mathrm{k}\begin{bmatrix}12(1-d_i) & 6(1-d_i)(1-d_j) & 0\\ 6(1-d_i)(1-d_j) & 12(1-d_j) & 0\\ 0 & 0 & \dfrac{EA(1-d_i)}{kL}\end{bmatrix} \tag{25}$$

$$k = \frac{1}{4-(1-d_i)(1-d_j)}\frac{EI}{L}$$

It can be observed that in the case where $\{\mathbf{D}_b\}$ is equal to zero, $[\mathbf{S}_b^d]$ reduces to the standard stiffness elastic matrix, $[\mathbf{S}_b^d(\mathbf{D}_b=\mathbf{0})] \Rightarrow [\mathbf{S}_b^e]$. If one of the bending concentrated damage variables takes value equal to one, while the other bending concentrated damage and the axial damage are equal to zero, then $[\mathbf{S}_b^d(\mathbf{D}_b)]$ becomes the stiffness matrix of an elastic member with an internal hinge at the end, on the left or the right.

For the case where both bending concentrated damage variables acquire values equal to one, while the axial damage is equal to zero, we obtain the stiffness matrix of an elastic truss bar where only the axial force remains. Furthermore, the stiffness matrix of a damaged member $[\mathbf{S}_b^d]$ obtained has the same shape as presented by Flórez-López (1999).

## 4.2. Damage evolution law

To apply the Continuum Damage Mechanics concepts to the frame analysis, it is necessary to adapt the theory as a function of the deformations at the hinges $i$ and $j$, as well as the deformation due to the elongation $\delta$. In addition, another necessary condition is that the variable evolutions should be independent of each other.

### *4.2.1. Free energy potential*

Extending the free energy definition $\boldsymbol{\Psi} = \frac{1}{2}\boldsymbol{\varepsilon}:\mathbf{C}:\boldsymbol{\varepsilon}$ (Malvern, 16), and redefining its as a function of generalized elastic deformations $\{\boldsymbol{\Phi}_b^e\}$ of one $b$ frame element and of it elastic stiffness matrix $[\mathbf{S}_b^e]$, we obtain the free energy potential as (Faleiro 2004)

$$\boldsymbol{\Psi}(\boldsymbol{\Phi}_b^e)=\boldsymbol{\Psi}_b^0=\frac{1}{2}\{\boldsymbol{\Phi}_b^e\}:[\mathbf{S}_b^e]:\{\boldsymbol{\Phi}_b^e\} \tag{26}$$

By rewriting (26) in terms of the rotations $\phi_i$ and $\phi_j$ at the ends of the element, as well as the elongation $\delta$, we obtain

$$\boldsymbol{\Psi}_b^0=\frac{1}{2}\left(4\frac{EI}{L}\phi_i+2\frac{EI}{L}\phi_j\right)\phi_i+\frac{1}{2}\left(4\frac{EI}{L}\phi_j+2\frac{EI}{L}\phi_i\right)\phi_j+\frac{1}{2}\frac{\mathrm{EA}}{\mathrm{L}}\delta^2 \tag{27}$$

In equation (27) we may observe that the free energy potential is the sum of the energies obtained by the rotations at the $i$ and $j$ nodes plus the elongation $\delta$, in such a way that the free energy potential can be redefined as (Faleiro 2004)

$$\boldsymbol{\Psi}_b^0=\boldsymbol{\Psi}_i^0+\boldsymbol{\Psi}_j^0+\boldsymbol{\Psi}_\delta^0 \tag{28}$$

Where

$$\boldsymbol{\Psi}_i^0=\frac{1}{2}\left(4\frac{EI}{L}\phi_i+2\frac{EI}{L}\phi_j\right)\phi_i \tag{29}$$

$$\boldsymbol{\Psi}_j^0=\frac{1}{2}\left(4\frac{EI}{L}\phi_j+2\frac{EI}{L}\phi_i\right)\phi_j \tag{30}$$

And

Structural Engineering

INTERSECTII

http://www.ce.tuiasi.ro/intersections

INTERSECTIONS



$$\mathbf{\Psi}_{\delta}^{0} = \frac{1}{2}\frac{EA}{L}\delta^{2} \ . \tag{31}$$

once, $m_i = 4\frac{EI}{L}\phi_i + 2\frac{EI}{L}\phi_j$, $m_j = 4\frac{EI}{L}\phi_j + 2\frac{EI}{L}\phi_i$, $n = \frac{EA}{L}\delta$, we can express $\mathbf{\Psi}_i^0$, $\mathbf{\Psi}_j^0$, and $\mathbf{\Psi}_{\delta}^0$ in terms of the moments at the ends and $m_j$, and the axial force $n$ as

$$\mathbf{\Psi}_i^0 = \frac{1}{2} m_i \phi_i \tag{32}$$

$$\mathbf{\Psi}_j^0 = \frac{1}{2} m_j \phi_j \tag{33}$$

$$\mathbf{\Psi}_{\delta}^0 = \frac{1}{2} n \delta \ . \tag{34}$$

*4.2.2. Energy norm for undamaged structure and damage evolution*

Now the undamaged energy norm vector $\tau^b$ is defined in the same way as the free energy; that is, as a function of the rotations $\phi_i$ and $\phi_j$ at the ends of the element and by the elongation $\delta$, following the (Simo 12) similarity formulation (Faleiro 2004)

$$\begin{aligned} \tau_i^b &= \sqrt{2\mathbf{\Psi}_i^0} = \sqrt{\left(4\frac{EI}{L}\phi_i + 2\frac{EI}{L}\phi_j\right)\phi_i} \\ \tau_j^b &= \sqrt{2\mathbf{\Psi}_j^0} = \sqrt{\left(4\frac{EI}{L}\phi_j + 2\frac{EI}{L}\phi_i\right)\phi_j} \\ \tau_{\delta}^b &= \sqrt{2\mathbf{\Psi}_{\delta}^0} = \sqrt{\frac{EA}{L}\delta^2} \end{aligned} \tag{35}$$

We then characterize the state of damage in the frame element by the means of a damage criterion, with the following functional form

$$\begin{aligned} g_i\left(\tau_i^b, r_i^b\right)_t &= \left(\tau_i^b\right)_t - \left(r_i^b\right)_t \le 0 \\ g_j\left(\tau_j^b, r_j^b\right)_t &= \left(\tau_j^b\right)_t - \left(r_j^b\right)_t \le 0 \\ g_{\delta}\left(\tau_{\delta}^b, r_{\delta}^b\right)_t &= \left(\tau_{\delta}^b\right)_t - \left(r_{\delta}^b\right)_t \le 0 \end{aligned} \tag{36}$$

Here, the subscript $t$ refers to value at current time $t \in \mathbb{R}_+$, $r_i^b, r_j^b$ and $r_{\delta}^b$ are the damage threshold at current time for the rotations $\phi_i$ and $\phi_j$ and the elongation $\delta$, respectively. We can consider the existence of one vector $r_0$, for $t = 0$, which denotes the initial damage threshold before any loading is applied, defined as

ISSN 1582-3024

Structural Engineering
INTERSECTII
INTERSECTIONS
http://www.ce.tuiasi.ro/intersections



$$\{r_0^b\} = \sqrt{\{\mathbf{M}_y\} : [\mathbf{S}_b]^{-1} : \{\mathbf{M}_y\}} = \begin{bmatrix} (r_i^b)_0 \\ (r_j^b)_0 \\ (r_\delta^b)_0 \end{bmatrix} \Rightarrow \begin{cases} (r_i^b)_0 = (r_j^b)_0 = \sqrt{\dfrac{L}{3EI} m_y{}^2} \\ (r_\delta^b)_0 = \sqrt{\dfrac{L}{EA} n_y{}^2} \end{cases} \quad (37)$$

where $m_y$ and $n_y$ are the bending moment and axial force limits. The vector $r_0$ can be considered as a property characteristic of the element, in way that we must have $r_t^b \geq r_0^b$.

Condition (equation (36)) states that damage in the element is initiated when the *energy norm* vector $\tau^b$ exceeds the initial damage threshold $r_0$. For the isotropic case, we define the evolution of the damage variables by

$$\dot{\mathbf{D}}_t^b = \dot{\lambda}^d H(\tau_t^b, \mathbf{D}_t^b) = \begin{cases} \dot{d}_i = \dot{\lambda}_i^d \left( (\tau_i^b)_t, d_i \right) \\ \dot{d}_j = \dot{\lambda}_j^d \left( (\tau_j^b)_t, d_j \right) \\ \dot{d}_a = \dot{\lambda}_\delta^d H\left( (\tau_\delta^b)_t, d_a \right) \end{cases} ; \dot{r}_t^b = \dot{\lambda}^d = \begin{cases} (\dot{r}_i^b)_t = \dot{\lambda}_i^d \\ (\dot{r}_j^b)_t = \dot{\lambda}_j^d \\ (\dot{r}_\delta^b)_t = \dot{\lambda}_\delta^d \end{cases} \quad (38)$$

where $\dot{\lambda}_i^d \geq 0$, $\dot{\lambda}_j^d \geq 0$ and $\dot{\lambda}_\delta^d \geq 0$ are *damage consistency* parameters that define damage loading/unloading conditions according to the Kuhn-Tucker relations

$$\begin{aligned} &\dot{\lambda}_i^d \geq 0; \quad g_i\left( (\tau_i^b)_t, (r_i^b)_t \right) \leq 0; \quad \dot{\lambda}_i^d g_i = 0 \\ &\dot{\lambda}_j^d \geq 0; \quad g_j\left( (\tau_j^b)_t, (r_j^b)_t \right) \leq 0; \quad \dot{\lambda}_j^d g_j = 0 \\ &\dot{\lambda}_\delta^d \geq 0; \quad g_\delta\left( (\tau_\delta^b)_t, (r_\delta^b)_t \right) \leq 0; \quad \dot{\lambda}_\delta^d g_\delta = 0 \end{aligned} \quad (39)$$

Let us now analyze the concentrated damage evolution at hinge $i$. Conditions (39) are standard for problems involving unilateral constraint. If $g_i < 0$, the damage criterion is not satisfied, and by condition $(39)_3$, $\dot{\lambda}_i = 0$, hence, the damage rule (38) implies that $\dot{d}_i = 0$ and no further damage occurs. If, on the other hand, $\dot{\lambda}_i^d > 0$, further damage (loading) is taking place, condition $(39)_3$ now implies that $g_i = 0$. In this event the value of $\dot{\lambda}_i$ can be determined by the damage consistency condition, i.e.

$$g_i\left( (\tau_i^b)_t, (r_i^b)_t \right) = \dot{g}_i\left( (\dot{\tau}_i^b)_t, (r_i^b)_t \right) = 0 \Rightarrow \dot{\lambda}_i^d = (\dot{\tau}_i^b)_t \quad (40)$$

Finally, $(r_i^b)_t$ can be given by the expression

$$\left(r_i^b\right)_t = \max\left\{\left(r_i^b\right)_0, \max_{s\in(0,t)}\left(\tau_i^b\right)_s\right\} \tag{41}$$

By applying to the other parameters, we obtain

$$r_t^b = \max\left\{r_0^b, \max_{s\in(0,t)}\left(\tau_\Phi^b\right)_s\right\} = \begin{cases} \max\left\{\left(r_i^b\right)_0, \max_{s\in(0,t)}\left(\tau_i^b\right)_s\right\} \\ \max\left\{\left(r_j^b\right)_0, \max_{s\in(0,t)}\left(\tau_j^b\right)_s\right\} \\ \max\left\{\left(r_\delta^b\right)_0, \max_{s\in(0,t)}\left(\tau_\delta^b\right)_s\right\} \end{cases} \tag{42}$$

If now we consider that $H(\tau_t^b, \mathbf{D}_t^b)$ in condition (38) is independent of the vector $\{\mathbf{D}_t^b\}$ and assuming that the existence of one function monotonic $G$, such that $H(\tau_t^b) = \partial G(\tau_t^b)/\partial(\tau_t^b)$, the damage criterion defined in (36) can now be rewritten in relation as a function of $G$, i.e. at hinge $i$, by $g_i\left(\tau_i^b, r_i^b\right)_t = G\left(\tau_i^b\right)_t - G\left(r_i^b\right)_t \le 0$. In this way, the flow rule (38) and loading/unloading conditions (39) become

$$\left\{\dot{\mathbf{D}}_t^b\right\} = \dot{\lambda}^d \frac{\partial G(\tau_t^b, r_t^b)}{\partial \tau_t^b} = \begin{cases} \dot{d}_i = \dot{\lambda}_i^d \dfrac{\partial G\left(\left(\tau_i^b\right)_t, \left(r_i^b\right)_t\right)}{\partial\left(\tau_i^b\right)_t} \\ \dot{d}_j = \dot{\lambda}_j^d \dfrac{\partial G\left(\left(\tau_j^b\right)_t, \left(r_j^b\right)_t\right)}{\partial\left(\tau_j^b\right)_t} \\ \dot{d}_a = \dot{\lambda}_\delta^d \dfrac{\partial G\left(\left(\tau_\delta^b\right)_t, \left(r_\delta^b\right)_t\right)}{\partial\left(\tau_\delta^b\right)_t} \end{cases} ;\quad \dot{r}_t^b = \dot{\lambda}^d = \begin{cases} \left(\dot{r}_i^b\right)_t = \dot{\lambda}_i^d \\ \left(\dot{r}_j^b\right)_t = \dot{\lambda}_j^d \\ \left(\dot{r}_\delta^b\right)_t = \dot{\lambda}_\delta^d \end{cases} \tag{43}$$

$$\begin{aligned} &\dot{\lambda}_i^d \ge 0; \quad g_i\left(\left(\tau_i^b\right)_t, \left(r_i^b\right)_t\right) \le 0; \quad \dot{\lambda}_i^d g_i = 0 \\ &\dot{\lambda}_j^d \ge 0; \quad g_j\left(\left(\tau_j^b\right)_t, \left(r_j^b\right)_t\right) \le 0; \quad \dot{\lambda}_j^d g_j = 0 \\ &\dot{\lambda}_\delta^d \ge 0; \quad g_\delta\left(\left(\tau_\delta^b\right)_t, \left(r_\delta^b\right)_t\right) \le 0; \quad \dot{\lambda}_\delta^d g_\delta = 0 \end{aligned} \tag{44}$$

Carrying through the integration in the time of the rate concentrated damage vector, the result is an expression that indicates the evolution of the damage variables as

$$\left\{\mathbf{D}_t^b\right\} = G\left(\tau_t^b\right) = \begin{cases} d_i = G\left(\left(\tau_i^b\right)_t\right) \\ d_j = G\left(\left(\tau_j^b\right)_t\right) \\ d_a = G\left(\left(\tau_\delta^b\right)_t\right) \end{cases} \tag{45}$$

ISSN 1582-3024

The function $G$ can be defined in relation with of the type of analysis. In our work, one expression used was the exponential softening proposed by Oller (2001)

$$G\left(\left(\tau_k^b\right)_t\right)=1-\frac{\left(\tau_k^b\right)_t}{\left(r_k^b\right)_0}e^{A\left(1-\frac{\left(r_k^b\right)_0}{\left(\tau_k^b\right)_t}\right)}\ ;\ A=\frac{1}{\frac{g_f}{\left(r_k^b\right)_0^2}-\frac{1}{2}}\ ;\ k\in\left(i,j,\delta\right)\ ; \quad (46)$$

where the parameter $g_f$ represents the fracture energy of the material, parameter derived from fracture mechanics as $g_f = G_f / l_c$, where $G_f$ is the fracture energy and $l_c$ can be defined as the characteristic length of the fractured member (Oller 2001) or alternatively as $l_c = \sqrt{A}$ where $A$ is the element section area (Salamy et al. 2005).

## 5. PLASTIC-DAMAGE MODEL FOR REINFORCED CONCRETE FRAMES

Elastic damage or elastic plastic laws are not sufficient to represent the constitutive behavior of reinforced concrete. In some damage models, during the loading/unloading process, a zero stress corresponds to a zero strain and the value of the damage is thus overestimated (Figure 2b).

An elastic plastic relation is not valid either, even with softening, (Figure 2a), as the unloading curve follows the elastic slope. A correct plastic-damage model should be capable of representing the softening behavior; the damage law reproduces the decreasing of the elastic modulus, while the plasticity effect accounts for the irreversible strains (Figure 2c). There are three ways to represent this behavior (Luccioni 2003):

One of these ways, based on a plastic-damage coupled model, evaluates the damage and the plastic behaviors at the same time. The free energy can be expressed as the sum of elastic energy with the plastic energy, both of them influenced by the damage parameter

$$\boldsymbol{\Psi}=\boldsymbol{\Psi}_e(\varepsilon,d)+\boldsymbol{\Psi}_p(\lambda^p,d) \quad (47)$$

Another option is to assume the free energy to be the sum of the elastic energy with the plastic energy and one term dependent of the damage. The result is that the dissipation energy is influenced by the damage parameter as the plasticity parameter

$$\boldsymbol{\Psi}=\boldsymbol{\Psi}_e(\varepsilon,d)+\boldsymbol{\Psi}_p(\lambda^p)+\boldsymbol{\Psi}_d(\lambda^d) \quad (48)$$

Structural Engineering

INTERSECTII

INTERSECTIONS

http://www.ce.tuiasi.ro/intersections



$$\Xi_d = \Psi \dot{d} - \lambda^p \lambda^d \tag{49}$$

The last option is to consider that damage and plasticity are uncoupled following their own laws independently; this way can be used when there are permanent deformations.

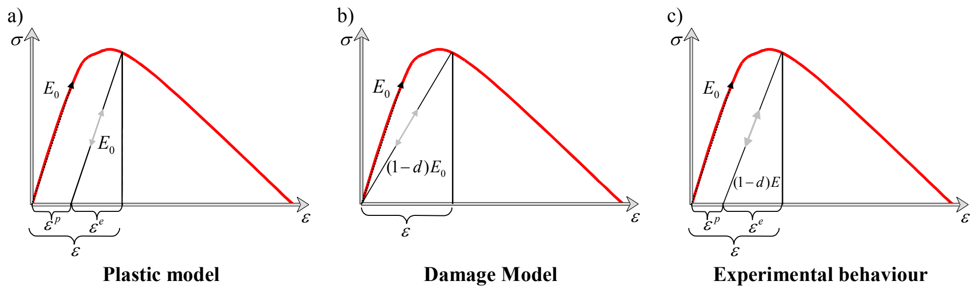


Figure 2. Loading-unloading behavior: simulated behaviors and experimental behavior

## 5.1. Plastic-damage model

### *5.1.1. Thermodynamic references*

As commented before, in the concrete of reinforced concrete elements, the damage effect modifies the constitutive plastic equation for small deformations by the degradation of the stiffness. New constitutive equation is formulated without time variation of temperature for thermodynamically stable problems, using the following mathematical formulation for the free energy constituted by elastic and plastic terms (Oller 2001, Faleiro et al. 2004)

$$\mathbf{\Psi}\left(\mathbf{\Phi}^e, \mathbf{D}, q^p, q^d\right) = \mathbf{\Psi}^e\left(\mathbf{\Phi}^e, \mathbf{D}, q^d\right) + \mathbf{\Psi}^p\left(q^p\right) \tag{50}$$

where $\mathbf{\Psi}^p$ is a plastic potential function and $\mathbf{\Psi}^e\left(\mathbf{\Phi}^e, \mathbf{D}, q^d\right)$ is the initial elastic stored energy. Additionally, $q^p$ and $q^d$ indicate the suitable set of internal (plastic and damage, respectively) variables and the elastic deformations $\{\mathbf{\Phi}^e\}$ is the free variable in the process.

For stable thermical state problems, the Clausius-Duhem dissipation inequality is valid and takes the form

$$\dot{\Xi} = \{\mathbf{M}\} : \{\dot{\mathbf{\Phi}}^e\} - \dot{\mathbf{\Psi}} \geq 0 \tag{51}$$

This inequality is valid for any loading-unloading stage. Taking the time derivative of equation (50) and substituting into (51) the following equation is obtained for dissipation

$$\dot{\Xi} = \left[ \{\mathbf{M}\} - \frac{\partial \Psi}{\partial \Phi^e} \right] : \{\dot{\Phi}\} + \frac{\partial \Psi}{\partial \Phi^e} : \{\dot{\Phi}^p\} - \frac{\partial \Psi}{\partial q^d} \dot{q}^d - \frac{\partial \Psi}{\partial q^p} \dot{q}^p \geq 0 \tag{52}$$

In order to guarantee the unconditional fulfilment of the Clausius-Duhem inequality, the multiplier of $\{\dot{\Phi}\}$ representing an arbitrary temporal variation of the free variable must be null. This condition provides the constitutive law of the damage problem

$$\left[ \{\mathbf{M}\} - \frac{\partial \Psi}{\partial \Phi^e} \right] \geq 0 \qquad \forall \{\dot{\Phi}\} \tag{53}$$

from where the final generalized stress of member can be defined as

$$\{\mathbf{M}_b\} = \frac{\partial \Psi_b}{\partial \Phi_b^e} \tag{54}$$

Once imposed the condition $\{\Phi_b^e\} = \{\Phi_b\} - \{\Phi_b^p\}$, the free energy for an elastic-plastic frame element with stiffness degradation can be written for small deformations as

$$\Psi_b\left(\Phi_b^e, \mathbf{D}_b, q^p, q^d\right) = \frac{1}{2}\left(\{\Phi_b\} - \{\Phi_b^p\}\right) : \left[\mathbf{S}_b^d\left(\mathbf{D}_b\right)\right] : \left(\{\Phi_b\} - \{\Phi_b^p\}\right) + \Psi_b^p\left(q^p\right) \tag{55}$$

where the stiffness matrix of the damaged member $\mathbf{S}_b^d\left(\mathbf{D}_b\right)$ is the same matrix defined in (25). By replacing this last equation in (54) one arrives at the expression for plastic-damage analysis (Cipollina et al. 1995, Flórez-López 1995, Faleiro et al. 2004)

$$\{\mathbf{M}_b\} = \left[\mathbf{S}_b^d\left(\mathbf{D}_b\right)\right] : \left(\{\Phi_b\} - \{\Phi_b^p\}\right) \tag{56}$$

## 6. MEMBER AND GLOBAL DAMAGE INDICES

### 6.1. Member damage index

The idea for the member damage index definition stemmed from a macroscale analogy with the continuous damage model definition. Thus, the starting point for deducing the member damage index is by the assumptions that we can express the free energy $\Psi_b$ of a member with the non-damaged free energy $\Psi_b^0$, defined in equation (31), as:

$$\Psi_b = (1 - D_b^M)\Psi_b^0 \tag{57}$$

ISSN 1582-3024

where $D_b^M$ is the member damage index. The free energy $\boldsymbol{\Psi}_b$ of a member can be defined in terms of the concentrated damage vector $\{\mathbf{D}_b\}$ as

$$\boldsymbol{\Psi}_b(\mathbf{D}_b) = \frac{1}{2}\{\boldsymbol{\Phi}_b\}:\left[\mathbf{S}_b^d(\mathbf{D}_b)\right]:\{\boldsymbol{\Phi}_b\} \tag{58}$$

considering

$$\left[\mathbf{S}_b^d(\mathbf{D}_b)\right]:\{\boldsymbol{\Phi}_b\} \cong \begin{Bmatrix}(1-d_i)m_i \\ (1-d_i)m_i \\ (1-d_i)m_i\end{Bmatrix} \tag{59}$$

and using (34) and (59), equation (58) can be rewritten as

$$\boldsymbol{\Psi}_b(\mathbf{D}_b) = (1-d_i)\boldsymbol{\Psi}_i^0 + (1-d_j)\boldsymbol{\Psi}_j^0 + (1-d_a)\boldsymbol{\Psi}_\delta^0 \tag{60}$$

Solving (57) for $D_b^M$, we obtain

$$D_b^M = 1 - \frac{\boldsymbol{\Psi}_b(\mathbf{D}_b)}{\boldsymbol{\Psi}_b^0} = 1 - \frac{(1-d_i)\boldsymbol{\Psi}_i^0 + (1-d_j)\boldsymbol{\Psi}_j^0 + (1-d_a)\boldsymbol{\Psi}_\delta^0}{\boldsymbol{\Psi}_i^0 + \boldsymbol{\Psi}_j^0 + \boldsymbol{\Psi}_\delta^0} \tag{61}$$

$$D_b^M = \frac{d_i\boldsymbol{\Psi}_i^0 + d_j\boldsymbol{\Psi}_j^0 + d_a\boldsymbol{\Psi}_\delta^0}{\boldsymbol{\Psi}_i^0 + \boldsymbol{\Psi}_j^0 + \boldsymbol{\Psi}_\delta^0} \tag{62}$$

which is the expression for member damage index for a frame member.

## 6.2. Global damage index

The global damage index can be defined as the sum of all free energy $\boldsymbol{\Psi}_b$ of a structure divided by the sum of the non-damaged free energy $\boldsymbol{\Psi}_b^0$

$$D_G = 1 - \frac{\sum_{b=1}^{3n}\boldsymbol{\Psi}_b(\mathbf{D}_b)}{\sum_{b=1}^{3n}\boldsymbol{\Psi}_b^0} = 1 - \frac{\sum_{b=1}^{3n}\{\boldsymbol{\Phi}_b\}:\left[\mathbf{S}_b^d(\mathbf{D}_b)\right]:\{\boldsymbol{\Phi}_b\}}{\sum_{b=1}^{3n}\{\boldsymbol{\Phi}_b\}:\left[\mathbf{S}_b^e\right]:\{\boldsymbol{\Phi}_b\}} \tag{63}$$

where $D_G$ is the global damage index. Replacing $\left[\mathbf{S}_b^e\right]\{\boldsymbol{\Phi}_b\} = \{\overline{\mathbf{M}}_b\}$, as well as $\left[\mathbf{S}_b^d(\mathbf{D}_b)\right]\{\boldsymbol{\Phi}_b\} = \{\mathbf{M}_b\}$, and assuming that $\{\boldsymbol{\Phi}_b\}^{\mathrm{T}} = \{\mathbf{U}\}^{\mathrm{T}}[\mathbf{B}_b]$, equation (63) becomes

$$D_G = 1 - \frac{\sum_{b=1}^{3n} \{\mathbf{\Phi}_b\} : \left[\mathbf{S}_b^d(\mathbf{D}_b)\right] : \{\mathbf{\Phi}_b\}}{\sum_{b=1}^{3n} \{\mathbf{\Phi}_b\} : \left[\mathbf{S}_b^e\right] : \{\mathbf{\Phi}_b\}} = 1 - \frac{\{\mathbf{U}\}^{\mathrm{T}} \sum_{b=1}^{3n} [\mathbf{B}_b]^{\mathrm{T}} \{\mathbf{M}_b\}}{\{\mathbf{U}\}^{\mathrm{T}} \sum_{b=1}^{3n} [\mathbf{B}_b]^{\mathrm{T}} \{\bar{\mathbf{M}}_b\}} \tag{64}$$

$$D_G = 1 - \frac{\{\mathbf{U}\}^{\mathrm{T}} \{\mathbf{F}_{int}^D\}}{\{\mathbf{U}\}^{\mathrm{T}} \{\mathbf{F}_{int}\}} \tag{65}$$

where $\{\mathbf{F}_{int}\}$ is the linear internal forces vector should the material preserve its original characteristics and undergo the actual deformation, and $\{\mathbf{F}_{int}^D\}$ is the nonlinear internal forces vector in the actual deformation. This global damage index is similar to that proposed by Hanganu et al. (2002) and Barbat et al. (1998) for finite element analysis.

The plastic and damage parameters can be calculated separately, as explained in Section 5. This assumption comes from the observation that damage is linked with the concrete, while plastification is related with the steel.

Table 1. Nonlinear time integration scheme (Newmark)

A. First iteration (passage from time instant $t$ to time instant $t+1$)
Update relevant matrices in the time $t$+1

$$\left[\mathbf{K}_t^{(1)}\right] = \sum_{b=1}^{nelements} \left[\mathbf{B}_b^T\right] : \left[\mathbf{S}_b^d\left(\mathbf{D}_b^{t-1}\right)\right] : [\mathbf{B}_b]$$

Compute:

$$\left\{\hat{\mathbf{F}}_{t+1}^{(1)}\right\} = \{\mathbf{F}_{ext}\} - \left[\mathbf{K}_t^{(1)}\right]\{\mathbf{U}_{t-1}\} \; ; \; \{\mathbf{D}\}_t^{(1)} = \{\mathbf{D}\}_{t-1} \quad ; \quad \{\mathbf{\Phi}^p\}_t^{(1)} = \{\mathbf{\Phi}^p\}_{t-1}$$

B. Loop over global convergence iterations: $n$th iteration
1.Calculate the first approximations for the iteration $n$:

$$[\mathbf{J}] = -\left|\frac{\partial \hat{\mathbf{F}}_t^{(n)}}{\partial \mathbf{U}_t^{(n)}}\right| ; \; \left\{\Delta \mathbf{u}_{t+1}^{(n)}\right\} = [\mathbf{J}]^{-1}\left\{\hat{\mathbf{F}}_t^{(n)}\right\} ; \; \left\{\mathbf{U}_t^{(n)}\right\} = \left\{\mathbf{U}_t^{(n-1)}\right\} + \left\{\Delta \mathbf{u}_t^{(n)}\right\}$$

2. Compute the member stresses and internal variables:

$$\{\mathbf{\Phi}_b\}_t^n = [\mathbf{B}_b]\left\{\mathbf{U}_t^n\right\} ; \; \{\mathbf{M}_b\}_t^n = \left[\mathbf{S}_b\left(\mathbf{D}_b\right)_t^n\right] : \left(\{\mathbf{\Phi}_b\}_t^n - \left\{\mathbf{\Phi}_b^p\right\}_t^n\right)$$

3.Updates relevant matrices

$$\left\{\mathbf{F}_{int}^D\right\}_t^{(n)} = \sum_{b=1}^{nelements} \left[\mathbf{B}_b^T\right] : \{\mathbf{M}_b\}_t^n \quad ; \left\{\hat{\mathbf{F}}_t^{(n)}\right\} = \{\mathbf{F}_{ext}\} - \left\{\mathbf{F}_{int}^D\right\}_t^{(n)}$$

3. If the residual forces norm $\left\|\hat{\mathbf{F}}_t^{(n)}\right\| / \left\|\mathbf{F}_{ext}(t)\right\| \le TOL$ , end of iterations and beginning of the computations in the next time step. If not, back to step 1 and proceed calculating.

ISSN 1582-3024

INTERSECTII
INTERSECTIONS
http://www.ce.tuiasi.ro/intersections



The global damage index, as well as member damage index, is basically tools for assessing the state of a structure. However, unlike the member damage index, which refers only to the damaged state of a member, the global damage index gives a measure of the structural stiffness loss, since the nonlinear internal forces $\{\mathbf{F}_{int}^{D}\}$ can be influenced not only by the damage but also by the plasticity.

## 7. NUMERICAL IMPLEMENTATION OF THE PLASTIC-DAMAGE MODEL

The most important results obtained by using the proposed model are: Deformations $\{\mathbf{\Phi}\}$, stresses $\{\mathbf{M}\}$, internal forces $\{\mathbf{F}_{int}\}$, plastic deformations $\{\mathbf{\Phi}^{p}\}$ or/and concentrated damage vector $\{\mathbf{D}\}$ the member damage index and global damage index and, if necessary, the remaining internal variables and their associated forces for each member of the structure.

These results are obtained by using the equilibrium equations (7) (quasi-static problems) together with the state law (56) in accordance with the internal variables evolution laws (16), and (44).

Table 1 shows the implicit Newmark time integration scheme used for quasi-static problems.

Let us now focus our attention on the calculation of the member stresses and of the internal variables (Table 1.B.2).

Therefore, the damage and the plastic evolution can be determined by the equations (35)-(45) for damage and equation (14)- for the plastic behavior. Table 2 shows the procedure for determining the parameters.

## 8. NUMERICAL EXAMPLES

### 8.1. Example 1: Model validation using a simple framed structure

The objective of this first example is to validate the proposed model and to evaluate the related concentrated damage and the global damage index of a structure. For this reason, we will analyze the results obtained by means of the proposal nonlinear frame analysis method in comparison with results obtained by means of a more refined finite element (FE) model.

The analyzed frame is 4 m high and 4 m wide loaded with two point forces (Figure 3a). The columns have a 8,43 cm x 5,62 cm cross section, the horizontal beam is 5,62 cm thick and 12,65 cm wide.

Table 2. Procedure to the determinations of the damage and plastic parameters

I. For each $b$ elements at $n$th iteration:

1. Generalized deformations at the step: $\{\boldsymbol{\Phi}_b\}_t^{(n)} = [\mathbf{B}_b]:\{\mathbf{U}\}_t^{(n)}$

2. Verification of the evolution of the damage:

i. Update of the internal variables: $\{\mathbf{D}_b\}_t^{(n)} = \{\mathbf{D}_b\}_t^{(n-1)}$ ; $\{\mathbf{r}_b\}_t^{(n)} = \{\mathbf{r}_b\}_t^{(n-1)}$

ii. Determination of the undamaged energy norm vector: $\boldsymbol{\tau}_\Phi^b = \sqrt{\{\boldsymbol{\Phi}_b\}_t^{(n)} : \mathbf{S}_b : \{\boldsymbol{\Phi}_b\}_t^{(n)}}$

iii. Verification of the evolution of the damage:

If $g\left(\tau_\Phi^b, (\mathbf{r}_b)_t^{(n)}\right) \le 0$ No damage evolution →3.

iv. Update of damage variable: $\{\mathbf{D}_b\}_t^{(n)} = G\left(\tau_\Phi^b\right)$

v. Update of damage threshold: $\{\mathbf{r}_b\}_t^{(n)} = \{\boldsymbol{\tau}_\Phi^b\}$

3. Verification of the evolution of the plastic variable:

i. Determination of generalized effective 'trial' stress and update of internal variables:

$\{\Delta\boldsymbol{\Phi}_b^p\}_0 = \{\boldsymbol{\Phi}_b^p\}_t^{(n-1)}$ ; $\{\Delta q^p\}_0 = \{q^p\}_t^{(n-1)}$

ii. Plastic evolution $k = k+1$:

$\{\bar{\mathbf{M}}_b^{trial}\}_k = [\mathbf{S}_b]:\left(\{\boldsymbol{\Phi}_b\}_t^{(n)} - \{\Delta\boldsymbol{\Phi}_b^p\}_{k-1}\right)$

iii. Verification of flow conditions and determination of plastic multiplier

$\left(\dot{\lambda}_i^p\right)_k = 0$ if $f\left[\left(\bar{m}_i^{trial}\right)_{k-1} - \left(\Delta q^p\right)_{k-1}\right]_i < 0$ or $\left(\lambda_i^p\right)_k \left[\dot{f}_i\right]_{k-1} < 0$

$\left(\dot{\lambda}_j^p\right)_k = 0$ if $f\left[\left(\bar{m}_j^{trial}\right)_{k-1} - \left(\Delta q^p\right)_k\right]_j < 0$ or $\left(\lambda_j^p\right)_k \left[\dot{f}_j\right]_{k-1} < 0$

No plasticity evolution →4.

$\left(\dot{\lambda}_i^p\right)_k \ne 0$ if $f\left[\left(\bar{m}_i^{trial}\right)_{k-1} - \left(\Delta q^p\right)_{k-1}\right]_i = 0$ or $\left(\lambda_i^p\right)_k \left[\dot{f}_i\right]_{k-1} = 0$

$\left(\dot{\lambda}_j^p\right)_k \ne 0$ if $f\left[\left(\bar{m}_i^{trial}\right)_{k-1} - \left(\Delta q^p\right)_{k-1}\right]_j = 0$ or $\left(\lambda_j^p\right)_k \left[\dot{f}_j\right]_{k-1} = 0$

Plastic evolution→3.iv

iv. Update of plastic variables and of the generalized effective 'trial' stress:

v. Back to 3.ii

4. End of the process of plastic correction

$\{\boldsymbol{\Phi}_b^p\}_t^{(n)} = \{\Delta\boldsymbol{\Phi}_b^p\}_k$ ; $\{q^p\}_t^{(n)} = \{\Delta q^p\}_k$

5. Achievement of the final generalized stress on the step $n$:

$\{\mathbf{M}_b\}_t^{(n)} = \left[\mathbf{S}_b\left(\mathbf{D}_b\right)_t^{(n)}\right]:\left(\{\boldsymbol{\Phi}_b\}_t^{(n)} - \{\boldsymbol{\Phi}_b^p\}_t^{(n)}\right)$

6. End of integration process of the constitutive equation.

Two FE models have been considered (Oller et al. 1996), the first one was modeled using the Timoshenko 3-noded beams elements to represent the structure (see Figure 3d) and the second was modeled using 75 2D 8-noded quadrilateral elements (see Figure 3e).

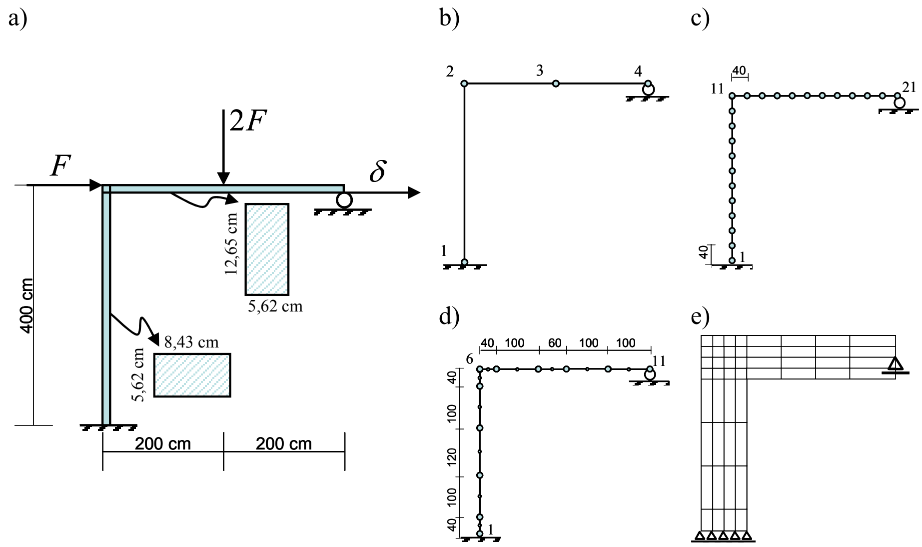


Figure 3. Geometry of the studied frame. a) Geometry and cross section b) numeration of the nodes of for frame with 3 elements , c) numeration of the nodes of for frame with 20 elements; d) FE mesh using Timoshenko 3-noded beams elements, e) FE mesh using 2D 8-noded quadrilateral elements

Three frames models have been considered; the first one the frame was discretized by only 3 frame elements, one to defines the column and two to defines the beam (see Figure 3a), the second frame the column and the beam are represented by 10 frame elements (see Figure 3c) and the in last frame, it was adopted the same division of the 3-noded beams elements described in Figure 3d.

In all cases, elastic modulus was $E = 2.110^5\,\text{MPa}$ while for the frame analysis it was assumed that the ultimate moment were $m_u = 45\,\text{kNm}$, for the beam, and $m_u = 20\,\text{kNm}$ for the column. The material was assumed a perfect elastoplastic law, such that, once reaches the elastic limit $\sigma_y = 200\,\text{MPa}$, it yields indefinitely at constant stress.

Figure 4 shows the results of the evolution of the force versus the displacement in the left upper corner of the frame obtained by each model, where we can notice that

Structural Engineering
INTERSECTII
INTERSECTIONS
http://www.ce.tuiasi.ro/intersections



the results obtained with the proposed frame analysis model are in a good agreement with the results obtained by using the FE model.

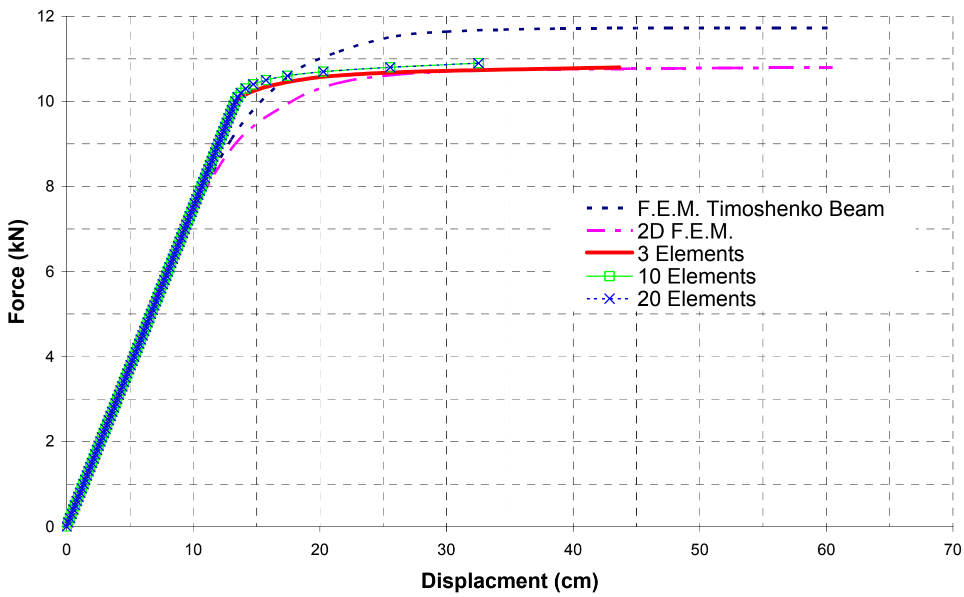


Figure 4. Comparison of the force-displacement curve for FEM results with results obtained by using the proposed plastic-damage model

The evolution of the moment at the column base is shown in Figure 5, where a comparison is made among the results obtained with the proposed method for different frame models.

The evolution of global damage index for each frame is shown in Figure 6. We also monitored the concentrated damage at the base and the top of the columns for each frame, once it is clearly expected that the structure will fail due to the weakening of the column. Studying together these three graphs we can analyze the behavior of each frame.

Observing the results in Figures 8 and 9 we can conclude that, although the concentrated damage effect in the frame analysis influences on the deformation and load capacity, it is the plasticity by means of the plastic hinges, and not the damage, what conditions the numerical stability of the structural analysis.

This behavior is in agreement with the assumptions that the structure continues to deform until the final instability is detected by the singularity of the global stiffness matrix, caused basically by the increment of the number of the plastic hinges in the frame than by the evolution of the damage.

ISSN 1582-3024

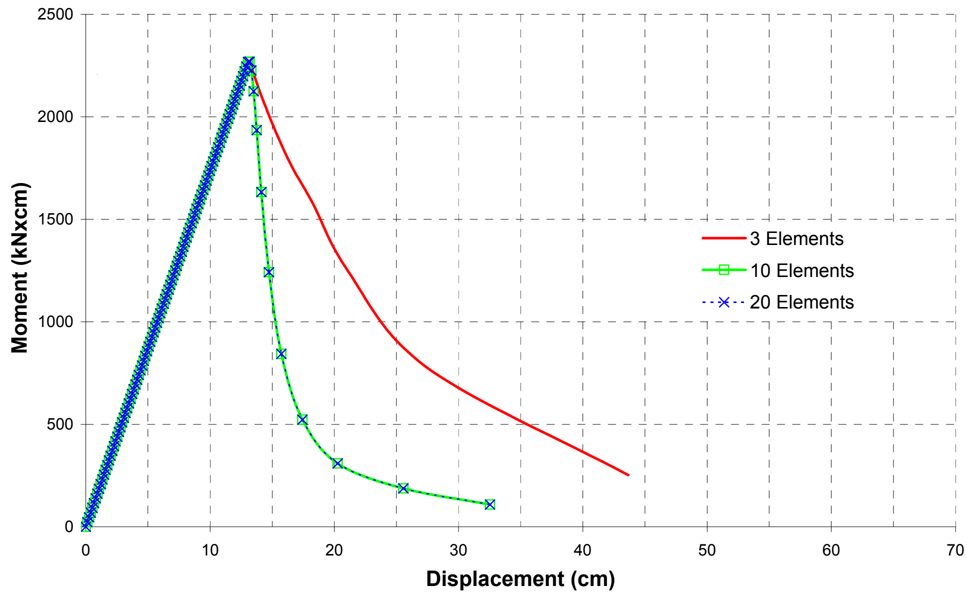


Figure 5. Moment on the column base versus displacement at the left upper corner

We can notice that before the concentrated damage beginning, all frames present a perfect plastic behavior, represented by a straight horizontal line (see Figure 5). When the analysis stops, at $\delta \cong 44\,\text{cm}$ for the 3 elements frame and at $\delta \cong 33\,\text{cm}$ for the others frames, the stiffness matrix becomes singular due to the presence of hinges (i.e, the nodes 3 and 1 in the first frame), and we can no longer perform the structural analysis.

This statement also can be confirmed by the fact that the damage at the column base is less than the global damage index for all cases (see Figure 5). The same curves are obtained for the frames modeled with 10 and 20 elements for both force-displacement relation (Figure 4), moment-displacement relation (Figure 5), global damage index evolutions and evolutions of the damage for the columns (see Figure 6).

Analyzing the damage in the frame modeled with 3 elements, the beginning of the concentrated damage at the top of the column is closer to the beginning of the concentrated damage at its base, and both have almost the same final value. Meanwhile, for the frame with 10 elements and with 20 elements, the damage at the top begins at very high loads while the damage at the base begins almost at the same instant when plasticity begins. In both frames the final value obtained for the concentrated damage at the base is higher than the value obtained at the top of the column.

ISSN 1582-3024

Structural Engineering
INTERSECTII
INTERSECTIONS
http://www.ce.tuiasi.ro/intersections



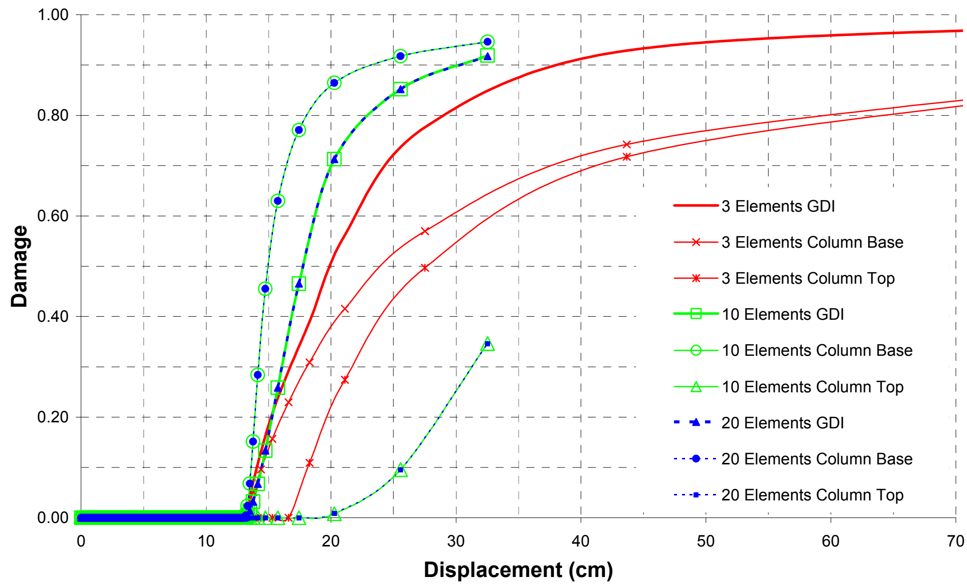


Figure 6. Evolution of the global damage index (GDI) and the concentrated damage at the base and at the top of the column

For the frame modeled with three elements, it can be seen clearly that the evolution of the global damage index is not related only due to the concentrated damage evolution but also to the plasticity evolution at the hinges.

We can also notice that for both the frames modeled with 10 elements and with 20 elements, the global damage index rapidly reaches high values for low deformations, what implies that the concentrated damage has more influence on the structural collapse than the plastic hinges, that is, the structure has little tendency to deform.

This can be due to the fact that the column and the beams are composed by several elements, dispersing the effect of the plasticity, while the damage is more concentrated at the base of the column. In conclusion, the behavior of the structure can be influenced by the number of elements and, therefore, the results obtained are smaller than it is expected.

### 8.2. Example 3: Model validation using a reinforced concrete framed structure

The objective of this example is to compare the results obtained by using the plastic-damage model described in this paper with the results of a quasi-static laboratory test performed by Vechio and Emara (1992) on a reinforced concrete frame.

Barbat et al. (1997) have already performed a numerical simulation of the behavior of the tested frame, but using a viscous damage model, implemented in a finite element program. A complete description of the geometrical and mechanical characteristics of the frame, as well as of the loads, is given in Figure 7.

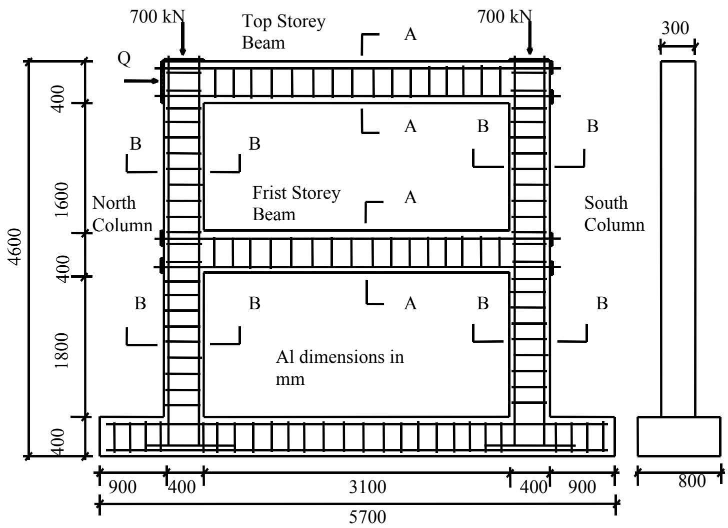


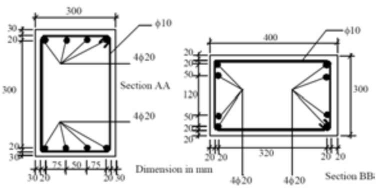


| Beams | Columns |
|---|---|
| *E=2.85E+7kN-m*<br>*A=0.12 m²,*<br>*I= 1.6E-3 m⁴*<br>*mcr=28 kNxm,*<br>*mp=189 kNxm* | *E=2.85E+7kN-m*<br>*A=0.12 m²,*<br>*I= 1.6E-3 m⁴*<br>*mcr=69 kNxm,*<br>*mp=253 kNxm* |

Figure 7. Description of the geometrical and mechanical characteristics of the frame of Example 3

The laboratory test consisted in applying a total axial load of 700 kN to each column and in maintaining this load in a force controlled mode throughout the test, which thus produced their pre-compression. A horizontal force was afterwards applied on the beam of the second floor, in a displacement-controlled mode, until the ultimate capacity of the frame was achieved (Vechio and Emara 1992).

In the numerical analysis of the frame the plastic constitutive equation used only takes into account the bending moments (equation (17)), while the lineal damage

Structural Engineering

INTERSECTII
http://www.ce.tuiasi.ro/intersections
INTERSECTIONS



equation proposed by Oller (2001) has been considered for determining the damage variable evolution, using in this case a fracture energy $G_f$ equal to $250\text{N/m}$ .

The curves in Figure 7 relate the horizontal forces and the displacements of the second floor beam and correspond to the load-unload laboratory test case and to the computer simulation using a viscous damage model (Barbat et al. 1997) and the plastic-damage model proposed in the present paper.

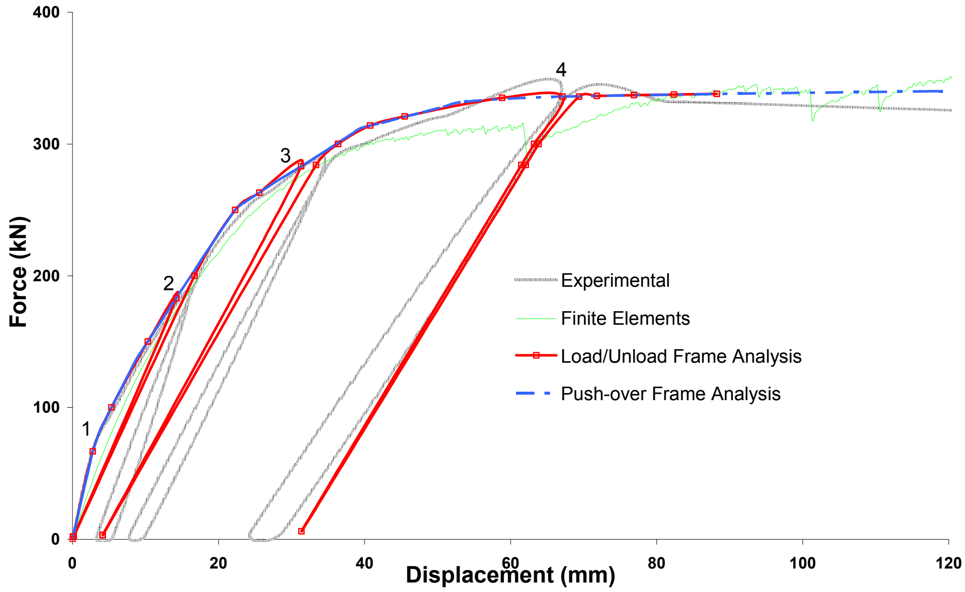


Figure 8. Comparison of the experimental results with results obtained by using the frame analysis with the proposed platic-damage model, and a finite element model.

The results are reasonably in agreement, taking into account the little computational effort required by the calculation of the model. In the first load-unload cycle, marked by point number two in Figure 8, the presence of residual deformations can be observed in the experimental curve, while in the numerical curve this does not occur. This is because the plastic-damage model still not reaches the plastic limit and the plastic deformations are assumed to occur only after the yielding of the reinforcement.

Nevertheless, when one of the elements reaches the plastic limit, it is possible to observe the influence of the plastic hinge on the curve. This situation is noticeable by the residual deformations represented in the subsequently unload-load cycles, at points three and four in Figure 8. However, in the laboratory test, non-negligible permanent deformations occurred before this, probably because of the inelastic strains and cracking of the concrete. A plastic-damage model taking into account

ISSN 1582-3024

this and other effects (such as confinement of the concrete, shear and dead loads) is under development.

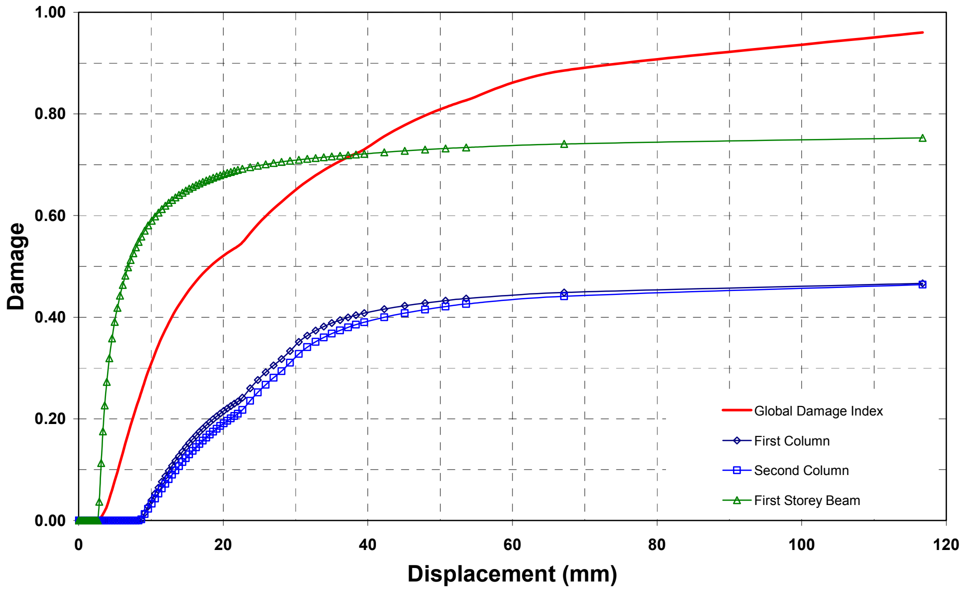


Figure 9. Evolution of the global damage and the member damage indexes at the first floor

Analyzing the damage evolution at the first floor, shown in Figure 9, and at the second floor, Figure 10, we can notice that the member damage begins in the first storey beam, followed almost simultaneously by damage of the second-story beam, after that, the damage in the first floor columns occurs and, finally, only after a considerable increase of the deformation, the damage begins in the second floor columns. This behavior is in agreement with the evolution of the damage observed in the laboratory test.

The effect of the damage in the first storey beam can also be detected in the force-displacement curve by the point 1 in Figure 8), which indicates the end of the elastic phase of the structure. However, in the first unload process of the frame, (point 2 in Figure 8) indicates that, at this moment, there is only damage in the frame model, aspect which is confirmed by the fact that the unload line returns to zero. At this point, as it was observed in the laboratory test, the damage occurs only at the first-story beam, at the second-story beam and at the columns of the first floor.

In the laboratory test, the structure looses stiffness because the propagation of the cracks throughout all the members at the point 2. However, in the frame analysis,

Structural Engineering

INTERSECTII
INTERSECTIONS
http://www.ce.tuiasi.ro/intersections



the structure looses stiffness only when the plastic effect begins, for loads closer to point 3, when yielding begins in the first floor at the base of both columns.

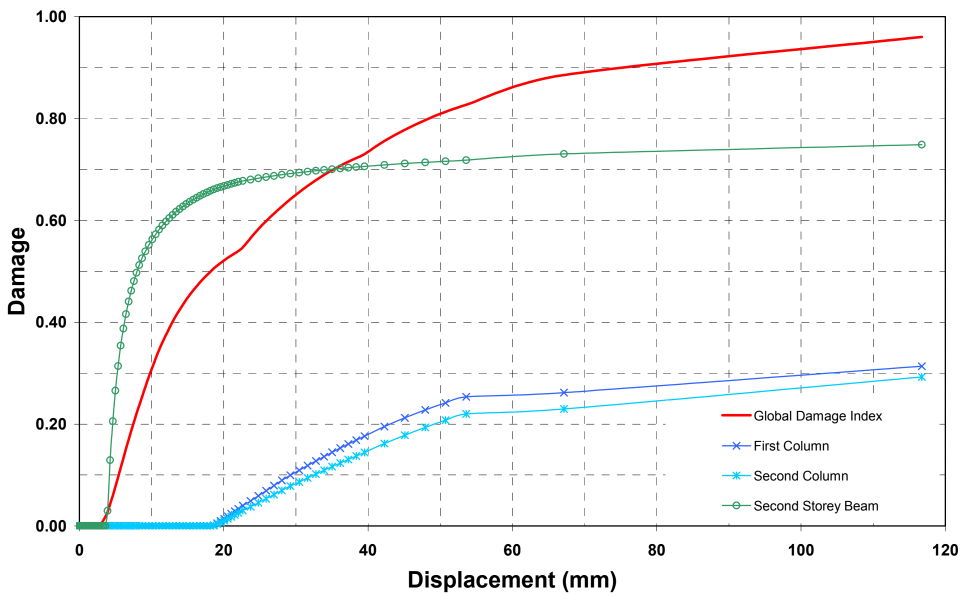


Figure 10. Evolution of the global damage and the member damage indexes at the second floor

In the laboratory test, the first yielding was detected at the bottom of the longitudinal reinforcement at the end of the first-story beam, followed by the yielding at the base of both columns of the first floor. In contrast, in the frame analysis the first yielding is detected at the base of both columns of the first floor, followed by the yielding of the first-story beam. These differences in the sequence of the yielding can be explained by the fact that in frame analysis the plastification of the end cross section of the members is sudden, and not gradual, or fiber-by-fiber, as observed in the first-story beam in the laboratory test.

The occurrence of the perfect plastic hinge at the first-storey beam and at the base of the first and second columns of the first floor implies a change of the static configuration for the whole structure, resulting in a slight change of the member damage indexes. This behavior can also be observed by the change in curvature of the global damage index curve. Physically, this can be interpreted as the failure of the concrete in compression of the first floor columns and of the beams and the ensuing redistribution of the stresses towards the steel.

J. Faleiro, A. Barbat, S. Oller

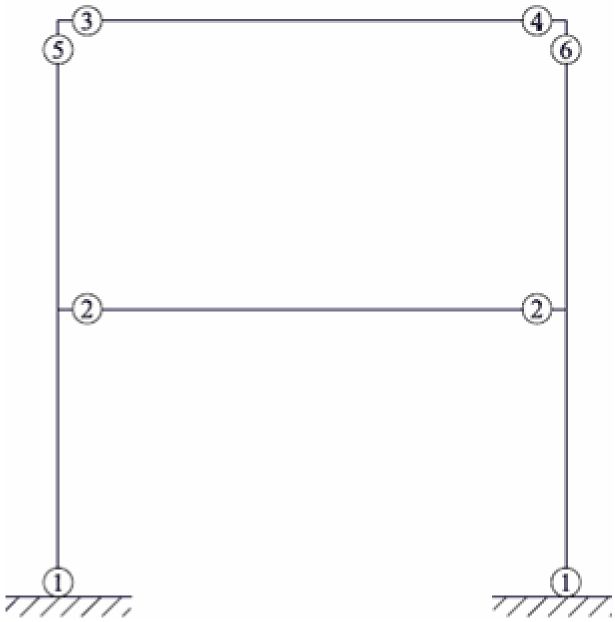


Figure 11. Sequence of formation of the plastics hinge within the frame

Figure 11 shows the sequence of formation of the plastic hinges in the frame analysis. Although it is different from the sequence observed in the laboratory test, the final result is the same. Nevertheless, the final deformation obtained in the frame analysis is less than in the laboratory tests because the structural analysis can no longer be perform due the presence of various plastic hinges.

## 9. CONCLUSIONS

A general framework for the nonlinear analysis of frames based on the Continuum Damage Mechanics and Plasticity Theory has been developed. The plastic-damage model developed in this paper assumes that plasticity and damage are uncoupled, have their own laws and that both are concentrated at ends of the frame members. Within this framework, many kinds of materials and loading conditions have been considered. Even the loading-unloading process has been simulated, and the values obtained provide satisfactory results when compared with laboratory tests, especially for reinforced concrete building.

The proposed model proves to be an effective tool for the numerical simulation of the collapse of frames. It could be a valuable alternative when other types of analyse, such as those based on multi-layer models, appear to be too expensive or

Structural Engineering

INTERSECTII INTERSECTIONS

http://www.ce.tuiasi.ro/intersections



impractical due to the size and complexity of the structure. The proposed model for reinforced concrete frames exhibited a very good precision confirmed by the examples included in the paper.

The global damage index has proved to be a powerful and precise tool for identifying the failure load and the structural mechanism leading to failure of reinforced concrete frame structures. This index, together with the member and the concentrated damage indexes, provides accurate quantitative measures for evaluating the state of any component of a damaged structure and of the overall structural behavior. It is an excellent tool for the seismic damage evaluation, reliability, and safety assessment of exiting structures and which can also be used in the evaluation of the repair or retrofitting strategies.

## References

1. A Hanganu, E. Oñate& A. Barbat, A finite element methodology for local/global damage evaluation in civil engineering structures. Computer and Structures, 80 (2002),pp. 1667-1687.
2. B. Luccioni, Apuntes de mecánica de daño continuo. Departamento de Resistencia de los Materiales y Estructuras a la Engeniería, Universidade Politécnica de Catalunya, 2003.
3. B. Luccioni, S. Oller & R. Danesi, Coupled plastic-damage model. Comput. Methods Appl. Mech. Engrg. 129 (1996),pp. 81-89
4. Barbat, M. Cervera, A. Hanaganu, C. Cirauqui, & E. Oñate, Failure pressure evaluation of the containment building of a large dry nuclear power plant. Nuclear Engineering and Design, 180 (1998), pp. 251-270.
5. C. Simo & J. Ju, Stress and strain based continuum damage models. Part I and II. Int. J. Solids Strucutres 23 (1987), pp. 821-869.
6. Cipolina, A. López Inojosa & J. Flórez-López, A simplified damage mechanics approach to nonlinear analysis of frames. Computer & Structures, 54 (1995) (6), pp. 1113-1126.
7. F. J. Vecchio & M. B. Emara, Shear deformations in reinforced concrete frames. ACI Structural Journal, 89, (1992)(1), pp. 45-46.
8. G. G. Deierlein, J. F. Hajjar & , A. Kavinde , Material nonlienar analysis of strucutres: a concentrated plasticity approach. Strucutural Engineering Report No. ST-01-10, Department of Civil Engineering, University of Minesota, 2001.
9. H. Barbat, S. Oller, E. Oñate & A. Hanganu, Viscous damage model for timoshenko beam structures. International Journal of Solids Structures, 34 (1997), ( 30), pp. 3953-3976.
10. J. C. Simo & T. J. R. Hughes , Computational Inelasticity. New York: Springer Verlag, 1998.
11. J. Faleiro, A. Barbat & S. Oller, (2005). Plastic Damage Model for Nonlinear Reinforced Concrete Frame Analysis. VIII International Conference on Computational Plasticity, COMPLAS VIII, 2 (2005),pp. 906-909.
12. J. Faleiro, A. Barbat & S. Oller, Aplicação de modelos de dano e plasticidade concentrado para o calculo matricial de estruturas de concreto armado. 47º Congresso Brasileiro do Concreto, 1 (2005), pp 201.
13. J. Faleiro, A. Barbat & S. Oller, Plasticidade e dano em pórticos de concreto Armado. 46º Congresso Brasileiro do Concreto, 1 (2004), pp 80-86
14. J. Flórez-López, Plasticidad y fractura en estructuras aporticadas. Monografías CIMNE, Barcelona, 1999.
15. J. Flórez-López, Simplified model of unilateral damage for reinforced concrete frames. Journal of Structural Engineering, ASCE. 121 (1995),p. 12.

ISSN 1582-3024

16. J. Flórez-López,. Modelos de daño concentrado para la simulación numérica del colapso de pórticos planos. Revista Internacional de Métodos Numéricos para Cálculo y Diseño en Ingeniería, 9 (1993) (2),pp. 123-139.
17. J.H. Argyris, B. Boni & M. Kleiber, Finite element analysis of two and three – dimensional elasto-plastic frames – the natural approach. Computer Methods in Applied Mechanics an Engineering, 35 (1982),pp. 221-248.
18. L. M. Kachanov, On Creep Rupture Time, Div. Eng. Sci., 8 (1958), pp. 26–31.
19. L. Malvern, Introduction to the mechanics of a continuos medium. Prentice Hall, Englewood Cliffs, 1969.
20. M. Jirásek & Z. P. Bazant, Inelastic analysis of structures. New York: John Willey & Sons, 2002
21. M. R. Salamy, H. Kobayashi & S. Unjoh, Experimental and analytical study on RC deep beams. Second International Conference on Concrete & Development, 2005.
22. M. S. Álvares, Aplicação de um modelo de dano localizado a estruturas de barras em concreto armado. Universidade Católica de Goiás <http://www.ucg.br>. Manuel_da_Silva_Álvares.pdf, jully 20, 2004.
23. M. S. Álvares, Estudo de um modelo de dano para o concreto: formulação indentificação paramétrica e aplicação com emprego do método dos elementos finitos. Departamento de Estruturas, Escola de Engenharia de São Carlos – USP, São Carlos, Brazil, 1993.
24. S. Oller, B. Luccioni & A. Barbat, Un Método de Evaluación del Daño Sísmico en Estructuras de Hormigón Armado. Revista Internacional de Métodos Numéricos para Cálculo y Diseño en Ingeniería, 12 (1996) (2),pp. 215-238.
25. S. Oller, Fractura mecánica – un enfoque global. CIMNE: Barcelona, 2001.
26. W. Chen, Plasticity in reinforced concrete. Mac Graw Hill, 1982.